American Journal of Quantum Chemistry and Molecular Spectroscopy
2017; 2(2): 18-27
http://www.sciencepublishinggroup.com/j/ajqcms
doi: 10.11648/j.ajqcms.20170202.11

Evaluation of the Physicochemical, Spectral, Thermal and Behavioral Properties of Sodium Selenate: Influence of the Energy of Consciousness Healing Treatment

Mahendra Kumar Trivedi[1], Alice Branton[1], Dahryn Trivedi[1], Gopal Nayak[1], William Dean Plikerd[1], Peter L. Surguy[1], Robert John Kock[1], Rolando Baptista Piedad[1], Russell Phillip Callas[1], Sakina A. Ansari[1], Sandra Lee Barrett[1], Sara Friedman[1], Steven Lee Christie[1], Su-Mei Chen Liu[1], Susan Elizabeth Starling[1], Susan Jones[1], Susan Mardis Allen[1], Susanne Kathrin Wasmus[1], Terry Ann Benczik[1], Thomas Charles Slade[1], Thomas Orban[1], Victoria L. Vannes[1], Victoria Margot Schlosser[1], Yusif Sarkis Yamin Albino[1], Kalyan Kumar Sethi[2], Parthasarathi Panda[2], Snehasis Jana[2, *]

[1]Trivedi Global, Inc., Henderson, USA

[2]Trivedi Science Research Laboratory Pvt. Ltd., Bhopal, India

Email address:

publication@trivedieffect.com (S. Jana)

[*]Corresponding author

To cite this article:

Mahendra Kumar Trivedi, Alice Branton, Dahryn Trivedi, Gopal Nayak, William Dean Plikerd, Peter L. Surguy, Robert John Kock, Rolando Baptista Piedad, Russell Phillip Callas, Sakina A. Ansari, Sandra Lee Barrett, Sara Friedman, Steven Lee Christie, Su-Mei Chen Liu, Susan Elizabeth Starling, Susan Jones, Susan Mardis Allen, Susanne Kathrin Wasmus, Terry Ann Benczik, Thomas Charles Slade, Thomas Orban, Victoria L. Vannes, Victoria Margot Schlosser, Yusif Sarkis Yamin Albino, Kalyan Kumar Sethi, Parthasarathi Panda, Snehasis Jana. Evaluation of the Physicochemical, Spectral, Thermal and Behavioral Properties of Sodium Selenate: Influence of the Energy of Consciousness Healing Treatment. *American Journal of Quantum Chemistry and Molecular Spectroscopy*. Vol. 2, No. 2, 2017, pp. 18-27. doi: 10.11648/j.ajqcms.20170202.11

Received: February 27, 2017; **Accepted**: May 2, 2017; **Published**: May 8, 2017

Abstract: Sodium selenate is an inorganic nutraceutical/pharmaceutical compound used for the prevention and treatment of several diseases. The current research article was aimed to explore the effect of The Trivedi Effect® - Energy of Consciousness Healing Treatment on the physicochemical, spectral, thermal, and behavioral properties of sodium selenate using PXRD, PSD, FT-IR, UV-vis, TGA, and DSC analysis. Sodium selenate was divided into two parts – one part was control, while another part was The Trivedi Effect® Treated sample which was received The Trivedi Effect® remotely by twenty renowned Biofield Energy Healers. A significant alteration of the crystallite size of the treated sample was observed in the range of -42.87% to 39.99% compared to the control sample. Consequently, the average crystallite size was significantly enhanced in the treated sample by 5.07% compared with the control sample. The particle size distribution of the treated sample at d_{10}, d_{50}, and d_{90} values were significantly reduced by 7.68%, 9.49%, and 4.08%, respectively compared with the control sample. Subsequently, the surface area of the treated sample was significantly increased by 8.16% compared with the control sample. The control and treated FT-IR spectra exhibited the sharp and strong vibration bands at 889 cm^{-1} and 888 cm^{-1}, respectively for Se=O stretching. The control and treated samples displayed the maximum absorbance at 204.9 nm and 204.5 nm, respectively. A significant reduction of total weight loss by 6.11% in the treated sample indicated the improvement of the thermal stability of the treated sample compared with the control sample. The vaporization temperature of the treated sample (95.68°C) was higher with a significant reduced latent heat of vaporization by 60.80% compared to the control sample (95.29°C). Thus, The Trivedi Effect® - Energy of Consciousness Healing Treatment might produce a new polymorphic form of sodium selenate which would be more soluble, dissolution rate, bioavailable, and thermally stable compared with the untreated sample. The Trivedi Effect® treated sodium selenate would be very suitable to design improved nutraceutical and pharmaceutical formulations that might provide better therapeutic response against several diseases such as stress, aging, inflammatory diseases, immunological disorders, infectious diseases, cancer, etc.

Keywords: Sodium Selenate, Energy of Consciousness Healing Treatment, Biofield Energy Healing Treatment, Biofield Energy Healers, The Trivedi Effect®, Particle Size, Surface Area, Thermal Analysis

1. Introduction

Sodium selenate is an inorganic nutraceutical used for selenium, an important micronutrient for normal metabolic reactions in the human body. Besides, selenium diminishes the toxic effect of heavy metals through forming the selenide complexes. It also protects from reactive oxygen species induced cell damages [1]. Selenium is found to be present in the active site of several enzymes and proteins [2]. For this reason, insufficiency of selenium is responsible for infertility, muscular dystrophy, leucocyte inefficiency, liver necrosis, etc. A little bit excess of selenium causes cancer, irritation of the skin, eye, deformation of hair and nails, depression, nervousness, etc. [2, 3]. Selenium has the four different oxidation states, *i.e.* -2, 0, +4, and +6 that affect its physicochemical properties like solubility and also availability to organisms. Selenate, the most oxidized form, is less toxic and highly soluble in water among selenium compounds [3, 4]. Thus, sodium selenate is used for the prevention and treatment of several diseases and disorders such as cancer, inflammatory diseases, Alzheimer's disease, diabetes, immunological disorders, etc. [5-8]. Sodium selenate can be used as insecticides and fungicides [9, 10]. Several methods such as the direct addition of selenium compounds to food, commercial fertilizers, media for plant growth and development, etc. are used for supplying selenium to our body [11]. Therefore, sodium selenate was used in a newly designed herbomineral formulation along with zinc chloride, magnesium gluconate, and *Withania somnifera* root extract used for the prevention and treatment of various human disorders and maintaining overall good health for better quality of life [12].

The biofield energy, which is a dynamic electromagnetic field existing surround of the human body is infinite, paradimensional, and can freely flow between human and environment that leads to the continuous movement or matter of energy [13, 14]. Healing practitioners have the power to harness this energy from the earth, the "universal energy field" and can be transmitted into the living and non-living substances by the Biofield Energy Healing Practitioners. The process of receiving the Biofield Energy Treatment and respond into useful way by the object is called as Biofield Energy Healing [15, 16]. Biofield (Putative Energy Fields) based Energy Therapies are used worldwide to promote health and healing. The National Center of Complementary and Integrative Health (NCCIH) has recognized and accepted Biofield Energy Healing as a Complementary and Alternative Medicine (CAM) health care approach in addition to other therapies, medicines and practices such as natural products, deep breathing, yoga, Tai Chi, Qi Gong, chiropractic/osteopathic manipulation, meditation, massage, special diets, homeopathy, progressive relaxation, guided imagery, acupressure, acupuncture, relaxation techniques, hypnotherapy, healing touch, movement therapy, pilates, rolfing structural integration, mindfulness, Ayurvedic medicine, traditional Chinese herbs and medicines, naturopathy, essential oils, aromatherapy, Reiki, cranial sacral therapy and applied prayer (as is common in all religions, like Christianity, Hinduism, Buddhism and Judaism) [17]. From the study on the various fields include materials science [18, 19], organic compounds [20, 21], microbiology [22, 23], agricultural [24, 25], genetics [26, 27], biotechnology [28, 29], nutraceuticals [30, 31], pharmaceuticals [32, 33], it has been proven that Biofield Energy Healing (also known as The Trivedi Effect®) has the astounding capability for alteration of the characteristic properties of the several non-living materials and living organisms. The literature reported that the bioavailability of inorganic selenium is lower than the organic forms of selenium such as selenium methionine which is also poorly absorbed from the gut of the human body [11]. The physicochemical properties such as particle size, crystalline structure, crystallite size, surface area, etc. of a drug play an important role in bioavailability, as these factors have direct influence on the absorption characteristic and stability of the drug [34]. The particle size, specific surface area, crystalline nature, chemical and thermal behavior of an atom/ion might be altered by The Trivedi Effect® through the possible mediation of neutrinos [35]. Powder X-ray diffraction (PXRD), particle size distribution analysis (PSD), Fourier transform infrared (FT-IR) spectrometry, ultraviolet-visible (UV-vis) spectroscopy, thermogravimetric analysis (TGA), and differential scanning calorimetry (DSC) analysis are useful analytical techniques for solving various problems encountered in industries for the pharmaceutical/nutraceutical formulation and developments [36]. Thus, the current study was aimed to evaluate the effect of the Biofield Energy Healing Treatment on the physicochemical, spectral, thermal, and behavioral properties of sodium selenate using various analytical techniques include PXRD, PSD, FT-IR spectrometry, UV-vis spectroscopy, TGA, and DSC.

2. Materials and Methods

2.1. Chemicals and Reagents

Sodium selenate was procured from Alfa Aesar, USA. All other chemicals used in the experiment were of analytical grade available in India.

2.2. Energy of Consciousness Healing Treatment Strategies

Sodium selenate was one of the components of the new proprietary herbomineral formulation, developed by our research team and it was used *per se* as the test compound

for the current study. The test compound was divided into two parts, one part of the test compound did not receive any sort of treatment and was defined as the untreated or control sodium selenate sample. The second part of the test compound was treated with The Trivedi Effect® - Energy of Consciousness Healing Treatment (Biofield Energy Treatment) by a group of twenty renowned Biofield Energy Healers remotely and was denoted as Biofield Energy Treated or The Trivedi Effect® Treated sample. Fifteen Biofield Energy Healers were remotely located in the U.S.A., two in Canada, one in the UK, one in Australia, and one in Germany, while the test compound was located in the research laboratory of GVK Biosciences Pvt. Ltd., Hyderabad, India. This Biofield Energy Treatment was provided for 5 minutes through Healer's Unique Energy Transmission process remotely to the test compound under the laboratory conditions. None of the Biofield Energy Healers in this study visited the laboratory in person, nor had any contact with the compounds. Similarly, the control compound was subjected to "sham" healers for 5 minutes, under the same laboratory conditions. The sham healer did not have any knowledge about The Trivedi Effect® - Energy of Consciousness Healing Treatment. After that, the treated and untreated samples were kept in similar sealed conditions and characterized thoroughly by PXRD, PSD, FT-IR, UV-visible spectroscopy, TGA, and DSC analysis.

2.3. Characterization

2.3.1. Powder X-ray Diffraction (PXRD) Analysis

The XRD analysis was accomplished on PANalytical X'Pert Pro powder X-ray diffractometer system. The XRD conditions and the sample preparation was followed as per the recent literature [37, 38]. The crystallite size (G) was calculated from the Scherrer equation [39]. The crystallite size (G) was calculated by using the following equation 1:

$$G = k\lambda/(b\cos\theta) \quad (1)$$

Where, k is the equipment constant (0.5), λ is the X-ray wavelength (0.154 nm); b in radians is the full-width at half of the peaks and θ the corresponding Bragg angle.

Percent change in crystallite size (G) was calculated using following equation (2):

$$\%\ \text{change in crystallite size} = \frac{[G_{Treated} - G_{Control}]}{G_{Control}} \times 100 \quad (2)$$

Where, $G_{Control}$ and $G_{Treated}$ are the crystallite size of the control and Biofield Energy Treated samples, respectively.

2.3.2. Particle Size Distribution (PSD) Analysis

The average particle size and particle size distribution were analyzed using Malvern Mastersizer 2000, UK with a detection range between 0.01 µm to 3000 µm. The PSD conditions and the sample preparation was followed as per the recent literature [37, 38].

The percent change in particle size (d) for at below 10% level (d_{10}), 50% level (d_{50}), and 90% level (d_{90}) was calculated using following equation (3):

$$\%\ \text{change in particle size} = \frac{[d_{Treated} - d_{Control}]}{d_{Control}} \times 100 \quad (3)$$

Where, $d_{Control}$ and $d_{Treated}$ are the particle size (µm) for at below 10% level (d_{10}), 50% level (d_{50}), and 90% level (d_{90}) of the control and Biofield Energy Treated samples, respectively.

Percent change in surface area (S) was calculated using following equation (4):

$$\%\ \text{change in surface area} = \frac{[S_{Treated} - S_{Control}]}{S_{Control}} \times 100 \quad (4)$$

Where, $S_{Control}$ and $S_{Treated}$ are the surface area of the control and Biofield Energy Treated samples, respectively.

2.3.3. Fourier Transform Infrared (FT-IR) Spectroscopy

FT-IR spectroscopy of sodium selenate was performed on Spectrum two (Perkin Elmer, USA) Fourier transform infrared spectrometer using pressed KBr disk technique [37, 38].

2.3.4. Ultraviolet-visible Spectroscopy (UV-Vis) Analysis

The UV-Vis spectral analysis was carried out using Shimadzu UV-2450 with UV Probe, Japan. The absorbance spectra and wavelength of maximum absorbance (λ_{max}) were recorded [37, 38].

2.3.5. Thermal Gravimetric Analysis (TGA)

TGA analysis was performed using instrument TGA Q50 (TA instruments, USA) and the remaining TGA conditions were followed as per the recent literature [37, 38]. The % change in weight loss (W) was calculated using following equation (5):

$$\%\ \text{change in weight loss} = \frac{[W_{Treated} - W_{Control}]}{W_{Control}} \times 100 \quad (5)$$

Where, $W_{Control}$ and $W_{Treated}$ are the weight loss of the control and Biofield Energy Treated samples, respectively.

2.3.6. Differential Scanning Calorimetry (DSC)

The analysis was performed using the DSC Q20 (TA Instruments, USA) using ~2.5 mg of samples. The remaining DSC conditions were followed as per the recent literature [37, 38]. The % change in melting point (T) was calculated using following equation (6):

$$\%\ \text{change in melting point} = \frac{[T_{Treated} - T_{Control}]}{T_{Control}} \times 100 \quad (6)$$

Where, $T_{Control}$ and $T_{Treated}$ are the melting point of the control and treated samples, respectively.

Percent change in the latent heat of fusion (ΔH) was calculated using following equation (7):

$$\%\ \text{change in latent heat of fusion} = \frac{[\Delta H_{Treated} - \Delta H_{Control}]}{\Delta H_{Control}} \times 100 \quad (7)$$

Where, $\Delta H_{Control}$ and $\Delta H_{Treated}$ are the latent heat of fusion of the control and treated samples, respectively.

3. Results and Discussion

3.1. Powder X-Ray Diffraction (PXRD) Analysis

The PXRD diffractograms of the both control and treated sodium selenate (Figure 1) showed very sharp and intense peaks indicating that both these samples were crystalline in nature. PXRD data such as Bragg angle (2θ), relative intensity (%), full width half maximum (FWHM) (θ°), and crystallite size (G) for the control and treated sodium selenate are presented in Table 1. The crystallite size was calculated by the help of Scherrer equation [39].

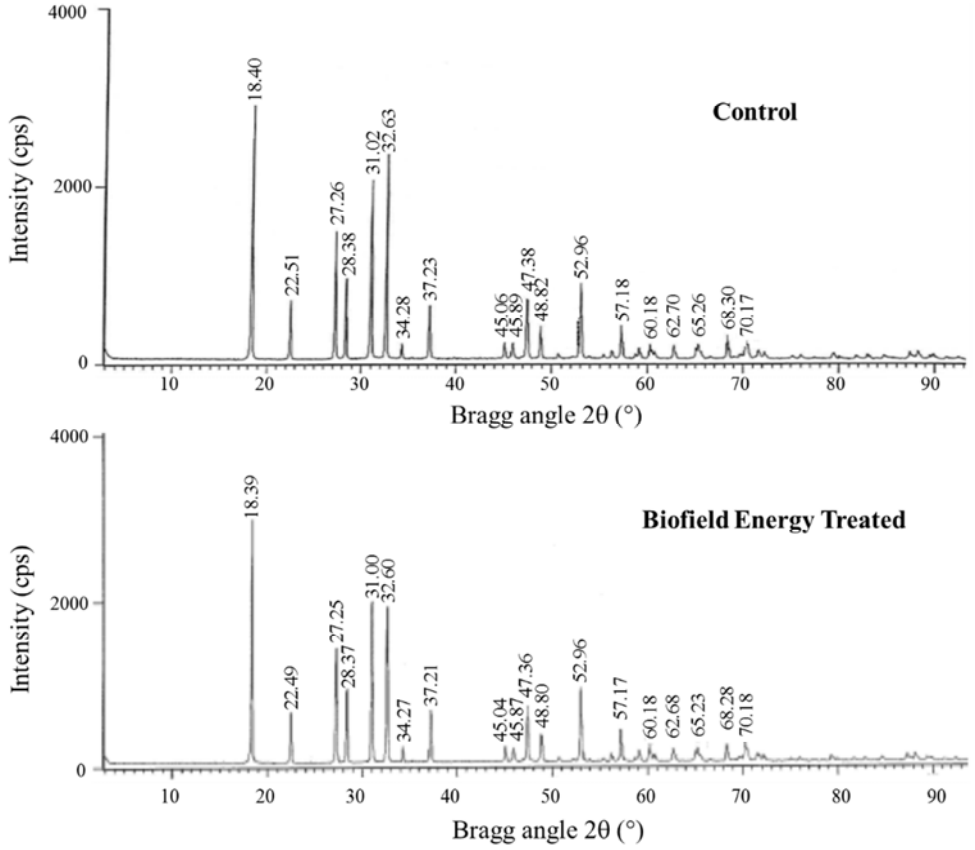

Figure 1. *PXRD diffractograms of the control and Biofield Energy Treated sodium selenate.*

Table 1. *PXRD data for the control and Biofield Energy Treated sodium selenate.*

Entry No.	Bragg angle (°2θ)		Relative Intensity (%)		FWHM (°2θ)		Crystallite size (G, nm)		
	Control	Treated	Control	Treated	Control	Treated	Control	Treated	% change*
1	18.40	18.39	100.00	100.00	0.1004	0.0836	44.41	53.34	20.09
2	22.51	22.49	23.21	21.04	0.1004	0.1171	44.70	38.33	-14.26
3	27.26	27.25	50.18	46.90	0.1338	0.1338	33.85	33.85	0.00
4	28.38	28.37	31.85	29.98	0.1004	0.1004	45.23	45.22	0.00
5	31.02	31.00	70.37	65.91	0.1171	0.1004	39.01	45.50	16.63
6	32.63	32.60	80.03	63.42	0.0816	0.0669	56.21	68.56	21.96
7	34.28	34.27	6.15	6.15	0.1020	0.0836	45.17	55.11	22.01
8	37.23	37.21	21.15	20.98	0.1632	0.1171	28.47	39.67	39.36
9	45.06	45.04	6.25	6.02	0.0836	0.0836	57.02	57.02	-0.01
10	45.89	45.87	5.96	5.87	0.1020	0.0836	46.88	57.19	22.00
11	47.38	47.36	23.39	22.30	0.1020	0.1020	47.14	47.14	-0.01
12	48.82	48.80	12.48	11.23	0.1020	0.1224	47.41	39.51	-16.67
13	52.96	52.96	29.54	36.70	0.1224	0.1020	40.20	48.24	20.00
14	57.18	57.17	13.01	19.57	0.1020	0.1224	49.18	40.98	-16.67
15	60.18	60.18	5.65	6.85	0.1020	0.0816	49.91	62.39	25.00
16	62.70	62.68	5.28	5.22	0.1428	0.1020	36.12	50.57	39.99
17	65.26	65.23	5.91	5.69	0.0816	0.1428	64.11	36.63	-42.87
18	68.30	68.28	9.03	6.48	0.1020	0.1020	52.20	52.19	-0.01
19	70.17	70.18	5.32	5.95	0.1224	0.1224	43.99	44.00	0.01
20	Average crystallite size						45.85	48.18	5.07

FWHM: Full width half maximum, *denotes the percentage change in the crystallite size of Biofield Energy Treated sample with respect to the control sample.

The PXRD diffractograms showed the notable changes of the crystallite size of the treated sodium selenate compared with the control sample. From Table 1 (entry 1), the most intense peaks for the control and treated samples were found at 2θ equal to 18.4°. The crystallite size of the Biofield Energy Treated sodium selenate at 2θ equal to nearly 18.4°, 31.0°, 32.6°, 34.3°, 37.2°, 45.9°, 52.3°, 60.2°, and 62.7° (Table 1, entry 1, 5-8, 10, 13, 15, and 16) were significantly increased from 16.63% to 39.99% with respect to the control sample. Consequently, at position 2θ equal to nearly 22.5°, 48.8°, 57.2°, and 65.3° (Table 1, entry 2, 12, 14, and 17), the crystallite sizes of the Biofield Energy Treated samples were significantly decreased in the range of 14.26% to 42.87% in comparison to the control sample. Besides, the crystallite size of the control and Biofield Energy Treated sodium selenate at 2θ equal to nearly 27.2°, 28.4°, 45.1°, 47.4°, 68.3°, and 70.2° (Table 1, entry 3, 4, 9, 11, 18, and 19) were same and not affected by the Biofield Energy Healing Treatment. Overall, the average crystallite size of the Biofield Energy Treated sodium selenate was increased by 5.07% as compared to the control sample. Beside these, other XRD parameters such as relative intensities of the PXRD peaks in the Biofield Energy Treated sodium selenate were significantly changed compared to the control sample. XRD relative intensity of each diffraction face on crystalline compound changes according to the crystal morphology [40]. Besides, alteration in the XRD pattern offers the proof of polymorphic transitions [41, 42]. Hence, changes in the crystallite size and relative intensities of XRD peaks revealed that the crystal morphology of the Biofield Energy Treated sample was modified from the control sample. Thus, it is anticipated that the change in the crystal morphology of the sodium selenate was due to the energy transferred through Biofield Energy Healing (The Trivedi Effect®) and this probably introduced a new polymorphic form of sodium selenate. Crystal habit, size and even polymorphic form of a drug have an important effect on drug solubility, dissolution, and bioavailability. Numerous examples in the scientific literature establish the impact of alteration in crystal morphology on *in vitro* dissolution rate, with prospective for improving bioavailability [43]. Thus, The Trivedi Effect® - Energy of Consciousness Healing Treatment might help for enhancing the bioavailability of sodium selenate.

3.2. Particle Size Distribution (PSD) Analysis

Particle size (d_{10}, d_{50}, and d_{90}) and surface area of the control and Biofield Energy Treated sodium selenate were explored, and the results are presented in Table 2. The particle size values of the control sodium selenate at d_{10}, d_{50}, and d_{90} were 5.08 µm, 24.14 µm, and 64.16 µm, respectively. The particle size values at d_{10}, d_{50}, and d_{90} of the Biofield Energy Treated sodium selenate were 4.69 µm, 21.85 µm, and 61.54 µm, respectively. Thus, the particle size values at d_{10}, d_{50}, and d_{90} of the Biofield Energy Treated sodium selenate were significantly decreased by 7.68%, 9.49%, and 4.08%, respectively with respect to the control sample. The surface area analysis demonstrated that the surface area of the Biofield Energy Treated sodium selenate (0.53 m^2/g) was significantly increased by 8.16% compared with the control sample (0.49 m^2/g).

Table 2. *Particle size data (d_{10}, d_{50}, and d_{90}) and surface area of the control and Biofield Energy Treated sodium selenate.*

Parameter	d_{10} (µm)	d_{50} (µm)	d_{90} (µm)	Surface area (m^2/g)
Control	5.08	24.14	64.16	0.49
Biofield Treated	4.69	21.85	61.54	0.53
Percent change* (%)	-7.68	-9.49	-4.08	8.16

*denotes the percentage change in the particle size data (d_{10}, d_{50}, and d_{90}) and surface area of Biofield Energy Treated sample with respect to the control sample.

The particle size, shape and surface area of the pharmaceuticals/nutraceuticals are essential for successful dosage form design and drug performance *i.e.* solubility, absorption, dissolution, and bioavailability [44]. Reduction in particle size and higher surface area enhance the solubility of the solid particles as well as increase the dissolution rate and bioavailability [45, 46]. Thus, it is predicted that The Trivedi Effect® - Energy of Consciousness Healing Treatment sodium selenate might be absorbed in faster rate from the gut and thus, can provide more bioavailability than the untreated sample.

3.3. Fourier Transform Infrared (FT-IR) Spectroscopy

The FT-IR spectra of the control and Biofield Energy Treated samples of sodium selenate are presented in Figure 2. The scientific literature reported that the water molecules, which are assimilated into the lattice structure of the crystalline inorganic compounds produce the characteristic absorption bands in the 3800-3200 cm^{-1} and 1700-1600 cm^{-1} regions due to the O-H stretching and bending for the water molecules, respectively [47]. The control IR spectrum displayed the O-H stretching and bending absorption bands at 3452, 1724, and 1643 cm^{-1}, respectively. In addition, peaks for the O-H stretching and bending of the water molecules in the Biofield Energy Treated sample were found at 3442, 1723, and 1643 cm^{-1}. The fingerprint region of the Biofield Energy Treated and control samples was remained unchanged. From the literature, it has been found that M=O (metal-oxide) stretching absorption band for inorganic materials was found in the 1010-850 cm^{-1} region [47]. A sharp and strong absorption bands at 889 cm^{-1} and 888 cm^{-1} due to the Se=O stretching were found in the spectrum of the control and Biofield Energy Treated sample, respectively. The analysis indicated that structure of the Biofield Energy Treated sodium selenate was remained close with respect to the control sample.

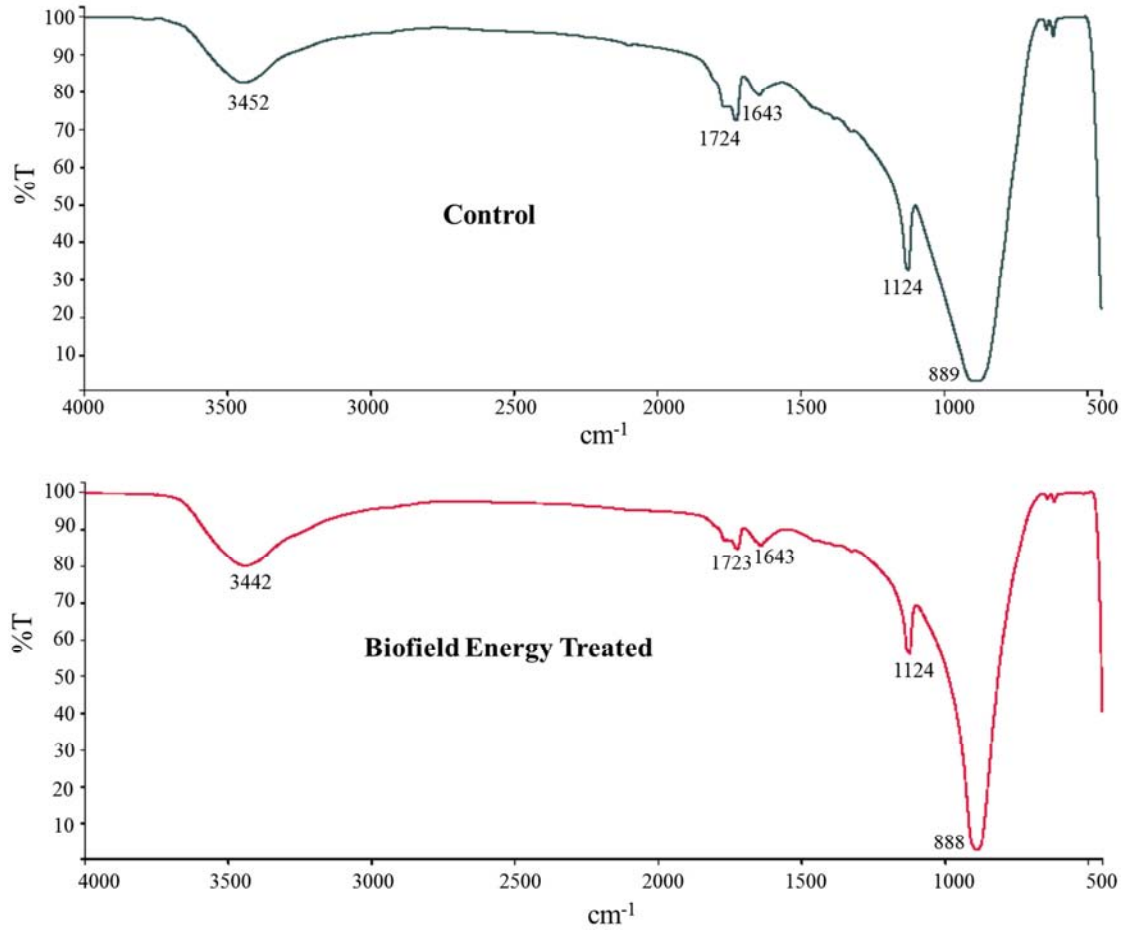

Figure 2. *FT-IR spectra of the control and Biofield Energy Treated sodium selenate.*

3.4. Ultraviolet-visible Spectroscopy (UV-Vis) Analysis

The UV-visible spectra of the both control and Biofield Energy Treated sodium selenate are shown in the Figure 3. The wavelength for the maximum absorbance (λ_{max}) of the control and Biofield Energy Treated sodium selenate were at 204.9 and 204.5 nm, respectively and there was a minor move of absorbance maxima from 2.4860 in the control sample to 2.4728 in the Biofield Energy Treated sample. However, the λ_{max} of the Biofield Energy Treated sample was remained unaffected in comparison with the control sample. The UV absorbance happens due to the different type of energy transitions from the singlet to the singlet excited state such as $\sigma \rightarrow \sigma^*$, $n \rightarrow \pi^*$, and $\pi \rightarrow \pi^*$. These type of electronic transitions occur when the difference in energy between the lowest unoccupied molecular orbital (LUMO) and the highest occupied molecular orbital (HOMO) is significantly greater than the activation energy of the compound [48]. As. there was no significant difference in the λ_{max} of the Biofield Energy Treated sample as compared to the control, it is anticipated that the structural configuration or activation energy of sodium selenate remained unaltered by the Biofield Energy Healing Treatment.

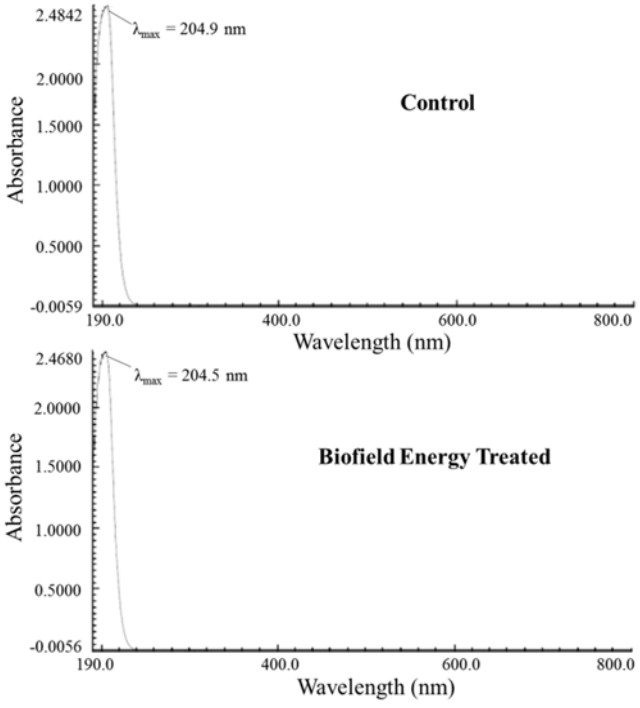

Figure 3. *UV-vis spectra of the control and Biofield Energy Treated sodium selenate.*

3.5. Thermal Gravimetric Analysis (TGA)

The thermal stability of a solid compound plays a vital role in the quality, efficacy, and safety in a drug formulation during the manufacturing process, shipment, storage, and handling [49]. Hence, TGA and DSC analysis were used to examine the thermal stability of both the control and Biofield Energy Treated sodium selenate. The TGA thermograms of both the control and Biofield Energy Treated samples, and their thermal analysis data are shown in Figure 4. The TGA analysis showed one steps of thermal degradation of sodium selenate.

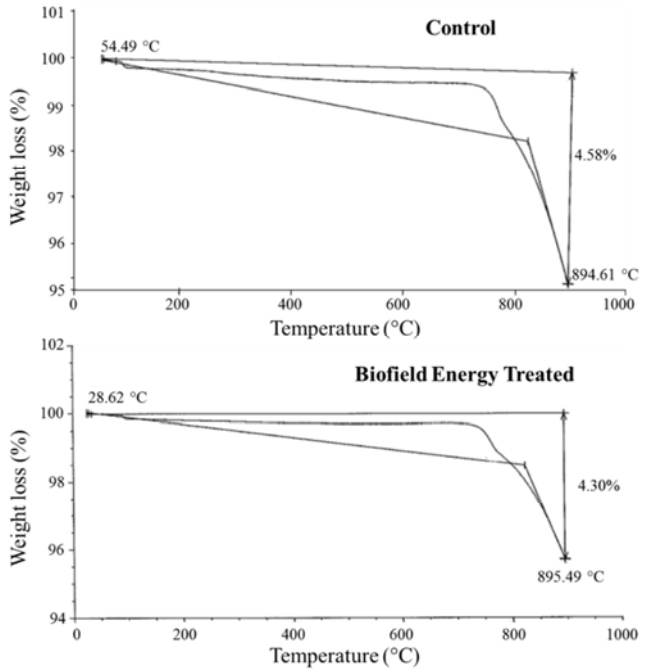

Figure 4. *TGA thermograms of the control and Biofield Energy Treated sodium selenate.*

The TGA thermogram of the control sample exhibited 4.58% weight loss from 54.49°C to 894.61°C. Consequently, the TGA thermogram of the Biofield Energy Treated sample showed 4.30% weight loss from 28.62°C to 895.49°C. The weight loss of the Biofield Energy Treated sample was significantly reduced by 6.11% compared to the control sample.

3.6. Differential Scanning Calorimetry (DSC) Analysis

The DSC thermograms of the control and Biofield Energy Treated sodium selenate are shown in Figure 5, and their DSC data are presented in Table 3. The DSC thermogram of the control sample showed the presence of a sharp endothermic peak at 95.29°C which was due to evaporation of the bound water and the latent heat of vaporization ($\Delta H_{vaporization}$) was 5.28 J/g. Consequently, the Biofield Energy Treated sodium selenate showed this endothermic peak at 95.65°C along with $\Delta H_{vaporization}$ of 2.07 J/g. This suggested that the temperature of the evaporation of the bound water in the Biofield Energy Treated sample was slightly (0.38%) increased, whereas the $\Delta H_{vaporization}$ was significantly decreased by 60.80% compared to the control sample. Therefore, it is assumed that The Trivedi Effect® - Energy of Consciousness Healing Treatment might improve the thermal stability of sodium selenate.

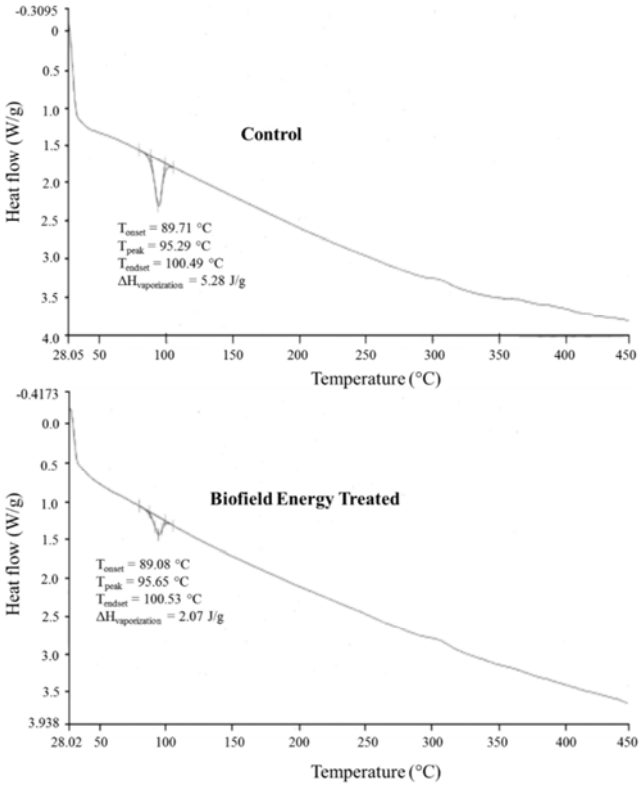

Figure 5. *DSC thermograms of the control and Biofield Energy Treated sodium selenate.*

Table 3. *Comparison of DSC data between the control and Biofield Energy Treated sodium selenate.*

Sample	T_{onset} (°C)	T_{peak} (°C)	T_{endset} (°C)	$\Delta H_{vaporization}$ (J/g)
Control	89.71	95.29	100.49	5.28
Biofield Energy Treated	89.08	95.65	100.65	2.07
% Change*	-0.70	0.38	0.16	-60.80

T_{onset}: Onset vaporization temperature, T_{peak}: Peak vaporization temperature, T_{endset}: Endset vaporization temperature, $\Delta H_{vaporization}$: Latent heat of vaporization, *denotes the percentage change of Biofield Energy Treated sample with respect to the control sample.

4. Conclusions

The Trivedi Effect® - Energy of Consciousness Healing Treatment (Biofield Energy Healing Treatment) has been found to be effective for altering the physicochemical, spectral, thermal, and behavioral properties of sodium selenate. The PXRD analysis displayed the significant alteration of the crystallite size of the treated sample from -42.87% to 39.99%

compared with the control sample. Thereafter, the average crystallite size of the treated sodium selenate was significantly increased by 5.07% indicating the alteration of the crystal morphology of the treated sodium selenate compared with the control sample. The particle size of the Biofield Energy Treated sample at d_{10}, d_{50}, and d_{90} values were significantly decreased by 7.68%, 9.49%, and 4.08%, respectively compared with the control sample. Therefore, the surface area of the treated sample was significantly increased by 8.16% compared with the control sample. TGA analysis revealed that the total weight loss of the Biofield Energy Treated sample was significantly reduced by 6.11% compared with the control sample. The DSC analysis showed that the vaporization temperature of the treated sample (95.68°C) was increased slightly compared to the control sample (95.29°C). The latent heat of vaporization was decreased significantly in the Biofield Energy Treated sample by 60.80% compared to the control sample. The TGA and DSC analysis revealed that Biofield energy Treated sample might have improved thermal stability compared with the control sample. Briefly, the Biofield Energy Treated sodium selenate might be a new polymorphic form of sodium selenate having increased crystallite size, decreased particle size with the enhanced surface area and thermal stability. Thus, The Trivedi Effect® treated sodium selenate could be more soluble, bioavailable, and would be very useful to design better nutraceutical and/or pharmaceutical formulations that might provide better the rapeutic response against various diseases such as diabetes mellitus, allergies, and septic shock, sleep disorder, insomnia, anxiety, depression, Attention Deficit Disorder, Attention Deficit Hyperactive Disorder, mental restlessness, brain frog, low libido, impotency, lack of motivation, mood swings, fear of the future, confusion, migraines, headaches, forgetfulness, overwhelm, loneliness, worthlessness, indecisiveness, frustration, irritability, chronic fatigue, obsessive/compulsive behavior and panic attacks, Lupus, Systemic Lupus Erythematosus, Hashimoto Thyroiditis, Diabetes, Asthma, Chronic peptic ulcers, Tuberculosis, Hepatitis, Chronic active hepatitis, Celiac Disease, Addison Disease, Crohn's disease, Graves' Disease, Anemia, Sjogren Syndrome, Irritable Bowel Syndrome, Multiple Sclerosis, Arthritis, Chronic periodontitis, Ulcerative colitis, Chronic sinusitis, Myasthenia Gravis, Atherosclerosis, Vasculitis, Dermatitis, Diverticulitis, Alopecia Areata, Psoriasis, Scleroderma, Fibromyalgia, Chronic Fatigue Syndrome, Vitiligo, Cardiovascular disease, cancer, Alzheimer's disease, Dementia, Cataracts, Osteoporosis, Hypertension, Glaucoma, Hearing loss, Parkinson's Disease, Huntington's Disease, Prion Disease, Motor Neuron Disease, Spinocerebellar Ataxia, Spinal muscular atrophy, Amyotrophic lateral sclerosis, Friedreich's Ataxia, Lewy Body Disease, chronic infections and much more.

Abbreviations

DSC: Differential scanning calorimetry, FT-IR: Fourier transform infrared spectroscopy, FWHM: Full width half maximum, G: Crystallite size, HOMO: Highest energy occupied molecular orbital, LUMO: Lowest energy unoccupied molecular orbital, TGA: Thermal gravimetric analysis, T_{onset}: Onset melting temperature, T_{peak}: Peak melting temperature, T_{endset}: Endset melting temperature, $\Delta H_{vaporization}$: Latent heat of vaporization, UV-vis: Ultraviolet-visible spectroscopy, PSD: Particle size distribution, PXRD: Powder X-ray diffraction.

Acknowledgements

The authors are grateful to GVK Biosciences Pvt. Ltd., Trivedi Science, Trivedi Global, Inc. and Trivedi Master Wellness for their assistance and support during this work.

References

[1] Fathi E, Farahzadi R (2013) Investigation of the effect of sodium selenate on acetylcholinesterase activity under extremely low frequency electromagnetic field. Journal of Biology and Life Science 4: 41-51.

[2] Soruraddin MH, Heydari R, Puladvand M, Zahedi MM (2011) A new spectrophotometric method for determination of selenium in cosmetic and pharmaceutical preparations after preconcentration with cloud point extraction. Int J Anal Chem 2011: 729651.

[3] Basnayake RST (2001) Inorganic selenium and tellurium speciation in aqueous medium of biological samples, Master of Science (Chemistry), December 2001, Sam Houston State University, Huntsville, Texas, 60 pp.

[4] Gonzalez CM, Hernandez J, Peralta-Videa JR, Botez CE, Parsons JG, Gardea-Torresdey JL (2012) Sorption kinetic study of selenite and selenate onto a high and low pressure aged iron oxide nanomaterial. J Hazard Mater 211-212: 138-145.

[5] Van Eersel J, Ke YD, Liu X, Delerue F, Kril JJ, Götz J, Ittner LM (2010) Sodium selenate mitigates tau pathology, neurodegeneration, and functional deficits in Alzheimer's disease models. Proc Natl Acad Sci USA 107: 13888-13893.

[6] Salama RM, Schaalan MF, Elkoussi AA, Khalifa AE (2013) Potential utility of sodium selenate as an adjunct to metformin in treating type II diabetes mellitus in rats: A perspective on protein tyrosine phosphatase. Biomed Res Int 2013: 231378.

[7] Ryan-Harshman M, Aldoori W (2005) The relevance of selenium to immunity, cancer, and infectious/inflammatory diseases. Can J Diet Pract Res 66: 98-102.

[8] Fleet JC (1997) Dietary selenium repletion may reduce cancer incidence in people at high risk who live in areas with low soil selenium. Nutr Rev 55: 277-279.

[9] Krieger RI (2001) Handbook of Pesticide Toxicology, 2nd Edn, Volume 1; Academic Press: San Diego, CA.

[10] Hanson B, Lindblom SD, Loeffler ML, Pilon-Smits E (2004) Selenium protects plants from phloem-feeding aphids due to both deterrence and toxicity. New Phytologist 162: 655-662.

[11] Haug A, Graham RD, Christophersen OA, Lyons GH (2007) How to use the world's scarce selenium resources efficiently to increase the selenium concentration in food. Microb Ecol Health Dis 19: 209-228.

[12] Trivedi MK, Branton A, Trivedi D, Nayak G, Balmer AJ, Anagnos D, Kinney JP, Holling JM, Balmer JA, Duprey-Reed LA, Parulkar VR, Gangwar M, Jana S (2016) Evaluation of pro-inflammatory cytokines expression in mouse splenocytes after incubation with biofield treated herbomineral formulation: effect of biofield energy healing treatment - The Trivedi Effect®. American Journal of Biomedical and Life Sciences. 4: 87-97.

[13] Rogers, M (1989) "Nursing: A Science of Unitary Human Beings." In J.P. Riehl-Sisca (ed.) Conceptual Models for Nursing Practice. 3rd Edn. Norwark: Appleton & Lange.

[14] Rosa L, Rosa E, Sarner L, Barrett S (1998) A close look at therapeutic touch. Journal of the American Medical Association 279: 1005-1010.

[15] Rubik B (2002) The biofield hypothesis: Its biophysical basis and role in medicine. J Altern Complement Med 8: 703-717.

[16] Nemeth L (2008) Energy and biofield therapies in practice. Beginnings 28: 4-5.

[17] Koithan M (2009) Introducing complementary and alternative therapies. J Nurse Pract 5: 18-20.

[18] Trivedi MK, Branton A, Trivedi D, Nayak G, Panda P, Jana S (2016) Evaluation of the isotopic abundance ratio in biofield energy treated resorcinol using gas chromatography-mass spectrometry technique. Pharm Anal Acta 7: 481.

[19] Trivedi MK, Branton A, Trivedi D, Nayak G, Sethi KK, Jana S (2016) Isotopic abundance ratio analysis of biofield energy treated indole using gas chromatography-mass spectrometry. Science Journal of Chemistry 4: 41-48.

[20] Trivedi MK, Branton A, Trivedi D, Nayak G, Bairwa K, Jana S (2015) Spectroscopic characterization of disodium hydrogen orthophosphate and sodium nitrate after biofield treatment. J Chromatogr Sep Tech 6: 282.

[21] Trivedi MK, Branton A, Trivedi D, Nayak G, Bairwa K, Jana S (2015) Fourier transform infrared and ultraviolet-visible spectroscopic characterization of ammonium acetate and ammonium chloride: An impact of biofield treatment. Mod Chem Appl 3: 163.

[22] Trivedi MK, Patil S, Shettigar H, Mondal SC, Jana S (2015) *In vitro* evaluation of biofield treatment on *Enterobacter cloacae*: Impact on antimicrobial susceptibility and biotype. J Bacteriol Parasitol 6: 241.

[23] Trivedi MK, Branton A, Trivedi D, Shettigar H, Nayak G, Gangwar M, Jana S (2015) Assessment of antibiogram of multidrug-resistant isolates of *Enterobacter aerogenes* after biofield energy treatment. J Pharma Care Health Sys 2: 145.

[24] Trivedi MK, Branton A, Trivedi D, Nayak G, Mondal SC, Jana S (2015) Morphological characterization, quality, yield and DNA fingerprinting of biofield treated alphonso mango (*Mangifera indica* L.). Journal of Food and Nutrition Sciences 3: 245-250.

[25] Trivedi MK, Branton A, Trivedi D, Nayak G, Gangwar M, Jana S (2015) Effect of biofield energy treatment on chlorophyll content, pathological study, and molecular analysis of cashew plant (*Anacardium occidentale L.*). Journal of Plant Sciences 3: 372-382.

[26] Trivedi MK, Branton A, Trivedi D, Nayak G, Gangwar M, Jana S (2015) Antibiogram and genotypic analysis using 16S rDNA after biofield treatment on *Morganella morganii*. Adv Tech Biol Med 3: 137.

[27] Trivedi MK, Patil S, Shettigar H, Bairwa K, Jana S (2015) Evaluation of phenotyping and genotyping characterization of *Serratia marcescens* after biofield treatment. J Mol Genet Med 9: 179.

[28] Trivedi MK, Branton A, Trivedi D, Nayak G, Mishra RK, Jana S (2015) Characterization of physical, thermal and spectral properties of biofield treated date palm callus initiation medium. International Journal of Nutrition and Food Sciences 4: 660-668.

[29] Trivedi MK, Patil S, Shettigar H, Bairwa K, Jana S (2015) Evaluation of phenotyping and genotyping characteristic of *Shigella sonnei* after biofield treatment. J Biotechnol Biomater 5: 196.

[30] Trivedi MK, Tallapragada RM, Branton A, Trivedi D, Nayak G, Latiyal O, Jana S (2015) Potential impact of biofield treatment on atomic and physical characteristics of magnesium. Vitam Miner 3: 129.

[31] Trivedi MK, Tallapragada RM, Branton A, Trivedi D, Nayak G, Latiyal O, Jana S (2015) Physical, atomic and thermal properties of biofield treated lithium powder. J Adv Chem Eng 5: 136.

[32] Trivedi MK, Branton A, Trivedi D, Nayak G, Bairwa K, Jana S (2015) Spectroscopic characterization of disulfiram and nicotinic acid after biofield treatment. J Anal Bioanal Tech 6: 265.

[33] Trivedi MK, Patil S, Shettigar H, Singh R, Jana S (2015) An impact of biofield treatment on spectroscopic characterization of pharmaceutical compounds. Mod Chem Appl 3: 159.

[34] Chereson R (2009) Bioavailability, bioequivalence, and drug selection. In: Makoid CM, Vuchetich PJ, Banakar UV (Eds) Basic pharmacokinetics (1st Edn) Pharmaceutical Press, London.

[35] Trivedi MK, Mohan TRR (2016) Biofield energy signals, energy transmission and neutrinos. American Journal of Modern Physics 5: 172-176.

[36] Chauhan A, Chauhan P (2014) Powder XRD technique and its applications in science and technology. J Anal Bioanal Tech 5: 212.

[37] Trivedi MK, Branton A, Trivedi D, Nayak G, Lee AC, Hancharuk A, Sand CM, Schnitzer DJ, Thanasi R, Meagher EM, Pyka FA, Gerber GR, Stromsnas JC, ShapiroJM, Streicher LN, Hachfeld LM, Hornung MC, Rowe PM, Henderson SJ, Benson SM, Holmlund ST, Salters SP, Panda P, Jana S (2017) Investigation of physicochemical, spectral, and thermal properties of sodium selenate treated with the Energy of Consciousness (The Trivedi Effect®). American Journal of Life Sciences 5: 27-37.

[38] Trivedi MK, Branton A, Trivedi D, Nayak G, Nykvist CD, Lavelle C, Przybylski DP, Vincent DH, Felger D, Konersman DJ, Feeney EA, Prague JA, Starodub JL, Rasdan K, Strassman KM, Soboleff L, Mayne MA, Keesee MM, Pillai PN, Ansley PC, Schmitz RD, Sodomora SM, Sethi KK, Panda P, Jana S (2017) Evaluation of the physicochemical, spectral, and thermal properties of sodium selenate treated with the Energy of Consciousness (The Trivedi Effect®). Advances in Bioscience and Bioengineering 5: 12-21.

[39] Langford JI, Wilson AJC (1978) Scherrer after sixty years: A survey and some new results in the determination of crystallite size. J Appl Cryst 11: 102-113.

[40] Inoue M, Hirasawa I (2013) The relationship between crystal morphology and XRD peak intensity on $CaSO_4.2H_2O$. J Crystal Growth 380: 169-175.

[41] Raza K, Kumar P, Ratan S, Malik R, Arora S (2014) Polymorphism: The phenomenon affecting the performance of drugs. SOJ Pharm Pharm Sci 1: 10.

[42] Brittain HG (2009) Polymorphism in pharmaceutical solids in Drugs and Pharmaceutical Sciences, volume 192, 2nd Edn, Informa Healthcare USA, Inc., New York.

[43] Blagden N, de Matas M, Gavan PT, York P (2007) Crystal engineering of active pharmaceutical ingredients to improve solubility and dissolution rates. Adv Drug Deliv Rev 59: 617-630.

[44] Khadka P, Ro J, Kim H, Kim I, Kim JT, Kim H, Cho JM, Yun G, Lee J (2014) Pharmaceutical particle technologies: An approach to improve drug solubility, dissolution and bioavailability. Asian J Pharm Sci 9: 304-316.

[45] Mosharrof M, Nyström C (1995) The effect of particle size and shape on the surface specific dissolution rate of microsized practically insoluble drugs. Int J Pharm 122: 35-47.

[46] Buckton G, Beezer AE (1992) The relationship between particle size and solubility. Int J Pharmaceutics 82: R7-R10.

[47] Stuart BH (2004) Infrared spectroscopy: Fundamentals and applications in Analytical Techniques in the Sciences. John Wiley & Sons Ltd., Chichester, UK.

[48] Hesse M, Meier H, Zeeh B (1997) Spectroscopic methods in organic chemistry, Georg Thieme Verlag Stuttgart, New York.

[49] Bajaj S, Singla D, Sakhuja N (2012) Stability testing of pharmaceutical products. J App Pharm Sci 2: 129-138.